tvst

Article

An In Vitro Bovine Cellular Model for Human Schlemm's Canal Endothelial Cells and Their Response to TGFβ Treatment

Jingwen Cai[1], Kristin Perkumas[2], W. Daniel Stamer[2,3], and Yutao Liu[1,4,5]

[1] Department of Cellular Biology and Anatomy, Augusta University, Augusta, GA, USA
[2] Department of Ophthalmology, Duke University, Durham, NC, USA
[3] Department of Biomedical Engineering, Duke University, Durham, NC, USA
[4] James & Jean Culver Vision Discovery Institute, Augusta University, Augusta, GA, USA
[5] Center for Biotechnology and Genomic Medicine, Augusta University, Augusta, GA, USA

Correspondence: Yutao Liu, 1460 Laney Walker Boulevard, CB1101, Augusta, GA 30912, USA. e-mail: yutliu@augusta.edu

Received: March 23, 2020
Accepted: May 17, 2020
Published: June 25, 2020

Keywords: glaucoma; POAG; IOP; Schlemm's canal; AAP; TGFβ

Citation: Cai J, Perkumas K, Stamer WD, Liu Y. An in vitro bovine cellular model for human schlemm's canal endothelial cells and their response to TGFβ treatment. Trans Vis Sci Tech. 2020;9(7):32, https://doi.org/10.1167/tvst.9.7.32

Purpose: Due to the limited availability of primary human Schlemm's canal (SC) endothelial cells, we aimed to develop an in vitro cellular model using the angular aqueous plexus (AAP) cells from bovine eyes.

Methods: We harvested a mixture of cells from the trabecular meshwork region including AAP loops from multiple donors, followed by puromycin treatment and immunostaining of Von Willebrand factor and vascular endothelial (VE)-cadherin to confirm identity. Previously identified differentially expressed genes in glaucomatous SC cells were examined in non-glaucomatous SC cells (n = 3) under 0% or 15% equibiaxial strain for 24 hours using droplet digital polymerase chain reaction (ddPCR) and analyzed using the Ingenuity Pathway Analysis (IPA) software application to identify upstream regulators. To compare the cellular responses to candidate regulators of these mechanoresponsive genes, AAP and human SC cells (n = 3) were treated with 5 or 10 ng/mL transforming growth factor beta-2 (TGFβ2) for 24 or 48 hours, followed with expression profiling using real-time PCR or ddPCR.

Results: We found that the isolated AAP cells displayed uniform cobblestone-like morphology and positive expression of two endothelial markers. In stretched SC cells, nine glaucoma-related genes were upregulated, and IPA implicated TGFβ as a potential upstream regulator. The effects of TGFβ2 treatment were similar for both AAP and SC cells in a dose- and time-dependent manner, activating *TGFBR1* and *SMAD2*, inhibiting *BMP4*, and altering expression of three glaucoma-related genes (*DCN, EZR,* and *CYP1B1*).

Conclusions: Bovine AAP cells may serve as an alternative cellular model of human SC cells.

Translational Relevance: These AAP cells may be used to study the functional pathways related to the outflow facility.

Introduction

Glaucoma is the leading cause of irreversible blindness worldwide.[1,2] Intraocular pressure (IOP) is the only modifiable major risk factor for glaucoma, and lowering IOP has proven to be an effective treatment to delay glaucoma progression.[3] The juxtacanalicular connective tissue (JCT) region, which is comprised of the inner wall of Schlemm's canal (SC) endothelium and adjacent trabecular meshwork (TM) cells, provides the majority of resistance to aqueous humor (AH) outflow and subsequently regulates IOP.[4,5] Compared to age-matched normal donor eyes, the stiffness of the intact JCT region and isolated primary cultures of SC cells is dramatically increased in glaucomatous eyes.[6–8]

These findings emphasize the important role of SC cells in glaucoma development and motivate their further study.

As the last barrier prior to AH drainage into systemic circulation, SC cells are under significant biomechanical stress due to the intraocular versus episcleral venous pressure gradient. This basal-to-apical pressure gradient manifests as dramatic cellular distention of SC cells, which form giant vacuoles when they lift off from their basal lamina and open pores.[9] Although the size and density of giant vacuoles are dependent on changes in IOP,[10] the pore density is also reduced in SC cells derived from glaucomatous eyes.[7] Because pore density can also change with controlled strains applied to SC cells in vitro, the stretch model is useful to study the biomechanics of SC cells in culture.[11]

Unfortunately, due to the anatomical location of SC cells and the technical difficulty associated with isolating sufficient numbers of cells, human SC cell studies have been limited.[12–14] Other attempts to explant dissected SC or to sort SC cells from TM mixed cultures using $CD31^+$ immunostaining were limited by the number of isolated cells and potential contamination from other cells.[9,15,16] Moreover, the limited availability and high cost of human donor eyes restrict those that can commit resources to routine isolations of SC cells.[17] Thus, it is necessary to establish an alternative cellular model for SC cell studies.

The anatomy and genetic background of non-human primates are similar to those of humans but the SC is even less accessible, and there have been no reports of successful isolation of SC cells. Like non-human primates, rodents have a similar SC, but the small size of the anterior chamber makes it even more difficult to isolate sufficient numbers of SC cells for study.[18,19] Bovine and porcine eyes have an anatomical variation of SC called the angular aqueous plexus (AAP). The identification of underlying JCT regions and micron-sized pores on the inner wall endothelial cells supports its equivalent function to SC.[20,21] The similarity and easy accessibility promote usages of bovine and porcine eyes in perfusion studies and outflow facility measurements.[22–24] Both SC and AAP cells are connected to each other by tight junctions, which serve to prevent the reflux of blood into the anterior chamber of the eye, similar to microvascular endothelial cells that function as blood–brain barriers.[25–27] Thus, a puromycin selection of AAP cells from porcine eyes was developed that takes advantage of increased expression of P-glycoprotein, a multidrug resistance efflux pump expressed in AAP cells but not neighboring TM cells.[28] Because access to porcine or bovine eyes can be limited depending on locations, and because our laboratory has access to bovine but not porcine eyes, we hypothesized that bovine AAP cells can also be differentially induced by P-glycoprotein and selected from TM cells by puromycin treatment, serving as an alternative in vitro cellular model for the functional pathway study of SC cells.

Table 1. Clinical Characteristics of Three Primary Human SC Endothelial Cell Donors

Cell Strain No.	Gender	Age (y)	Glaucoma
SC69	Male	45	No
SC70	Male	42	No
SC71b	Male	44	No

Methods

SC Cell Isolation and Culture

Human SC cells were isolated from three normal donor eyes within 36 hours of death, with enucleation occurring $\leq$6 hours after death according to the established techniques[14] (Table 1). These cells were cultured in complete culture medium containing low-glucose Gibco Dulbecco's Modified Eagle Medium (DMEM; Thermo Fisher Scientific, Waltham, MA), 10% fetal bovine serum (R&D Systems, Minneapolis, MN), 100-U/mL penicillin, and 100-µg/mL streptomycin (Gibco). Primary SC cells were maintained at 37°C in humidified air containing 5% CO_2 and passaged at a ratio of 1:3. All SC cell strains were characterized by positive staining of endothelial marker vascular endothelial (VE)-cadherin, a net transepithelial electrical resistance $\geq$ 10 ohms$\cdot$cm^2, and negative myocilin induction with dexamethasone to exclude mixtures of trabecular meshwork cells.[29] All cells were tested between the third and fifth passage and treated before passage six.

Stretch Assay

Three primary SC cell strains were used in stretch experiments that involved dividing the cells into non-stretched and stretched groups with duplicates. Cells were loaded onto six-well BioFlex culture plates (Flexcell International Corporation, Burlington, NC) coated with collagen type I. Plates were inserted in the Flexcell FX-5000 Tension System and either were stretched by 15% equibiaxial strain at 1 Hz or remained non-stretched for 24 hours. Total RNA was extracted using the *mir*Vana miRNA Isolation Kit (Thermo Fisher Scientific). RNA quality and quantity were evaluated using an Agilent Bioanalyzer 2100 with RNA 6000 Pico Chips (Agilent Technologies, Santa

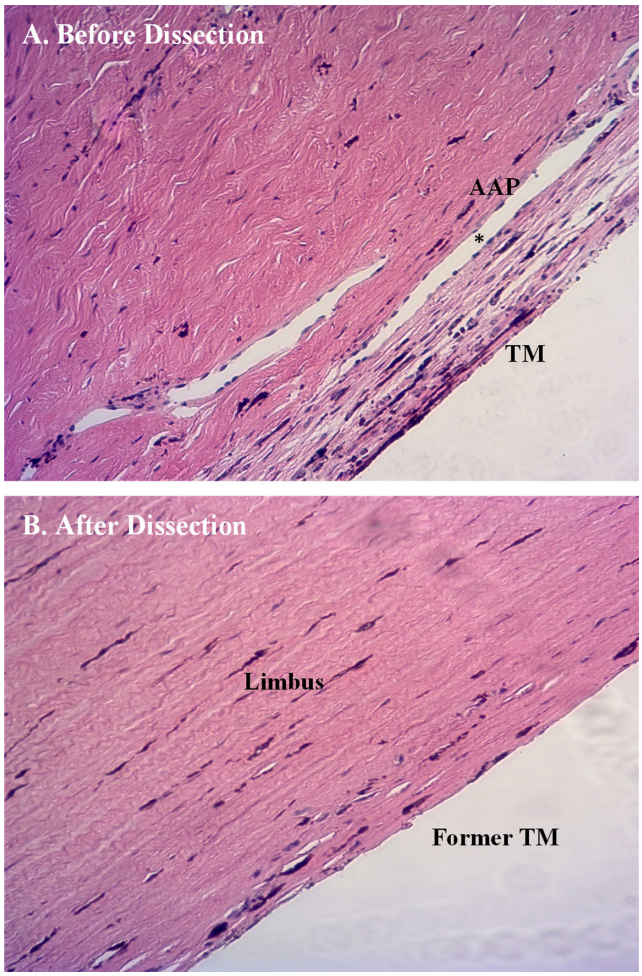

Figure 1. H&E stained sections of the anterior segment from bovine eyes before and after removal of the ciliary body and iris. (A) A sample before dissection of the trabecular meshwork (TM) and angular aqueous plexus (AAP) region. (B) A sample after removal of the trabecular meshwork and aqueous plexus tissue. Asterisk shows location of aqueous plexus lumen.

Clara, CA). All RNA samples had high RNA integrity number scores > 8.5, indicating good quality for downstream expression analyses.

Gene Expression Profiling

Isolated total RNA from stretched and non-stretched human SC cells was reverse transcribed to cDNA using the SuperScript IV First-Strand cDNA Synthesis System (Thermo Fisher Scientific) according to the manufacturer's recommended protocols. Droplet digital polymerase chain reaction (ddPCR) EvaGreen-based expression assays for specific human genes were obtained from Bio-Rad Laboratories, Inc. (Hercules, CA) (Table 2). The Bio-Rad QX200 ddPCR system was used to generate and measure the partitioned droplets for absolute quantification (copies/20 µl) of target genes as previously described.[30] *GAPDH* and *HPRT1* were used as the internal reference genes to normalize the gene expression across different samples.

Ingenuity Pathway Analysis

Differentially expressed genes in stretched SC cells were uploaded to the "My Pathway" function in the Ingenuity Pathway Analysis (IPA) software application (QIAGEN, Hilden, Germany) to determine potential relationships. Pathways and upstream regulators were ranked by *P* value according to the possibility of genes being altered simultaneously. Additionally, we generated a merged and customized network in accordance with known associations between genes to connect the genes of interest and examine the primary factors that play a role in response to the mechanical strain of SC cells.

Isolation and Culture of Bovine Outflow Cells

Bovine eyes from 1- to 2-year-old cows were obtained from a local slaughterhouse and stored on ice for up to 24 hours until dissection. Tissues outside the globes, such as fat, muscles, connective tissue, and optic nerve, were removed, and the globes were disinfected in 10% betadine solution (Purdue Pharma, New York, NY). The eyes were cut into halves using surgical scissors to remove the vitreous humor, lens, ciliary body, and iris. Under a dissecting microscope (Laxco MZS32; Fisher Scientific, Pittsburgh, PA), the iris root was carefully scraped away using a surgical blade to expose the groove where the TM and AAP are located. The tissue in the groove was removed by blunt dissection using a 1.5-mm curette. The hemotoxylin and eosin (H&E) staining histology slides showed our collection of TM region containing AAP tissue (Fig. 1). Tissues were pooled (n = 6) in the medium containing high-glucose DMEM complemented with 5% fetal bovine serum (Atlanta Biologicals), 5% newborn calf serum (Gibco), 5-mM L-glutamine (Gibco), 10-µg/mL endothelial cell growth factor, 90-µg/mL heparin, 2.5-µg/mL amphotericin B (Sigma-Aldrich, St. Louis, MO), 100-U/mL penicillin, 100-µg/mL streptomycin, and 50-µg/mL gentamicin (Gibco). The pooled tissue was digested by 1-mg/mL collagenase I (Sigma-Aldrich) in complete medium at 37°C for 1 hour and then centrifuged at 300*g* for 5 minutes to pellet the cells. The supernatant was aspirated and the pellet was washed with complete culture medium through another 300*g* centrifugation for 5 minutes. The cell pellet was resuspended and filtered through a 40-µm cell strainer (Corning, Inc.,

Table 2. Selected Bio-Rad ddPCR Human Gene Expression Assays

Gene Symbol	Gene Description	Bio-Rad Assay ID	Amplicon Size (bp)
ABCA1	ATP-binding cassette subfamily A member 1	dHsaEG5022809	85
BMP4	Bone morphogenetic protein 4	dHsaEG5001721	127
CAV1	Caveolin 1	dHsaEG5024315	107
CAV2	Caveolin 2	dHsaEG5002420	65
CDH2	Cadherin 2	dHsaEG5020622	151
CLDN23	Claudin 23	dHsaEG5005462	172
CYP1B1	Cytochrome P450, family 1, subfamily B, polypeptide 1	dHsaEG5019693	139
DCN	Decorin	dHsaEG5004873	133
EZR	Ezrin	dHsaEG5021343	60
GAS7	Growth arrest-specific 7	dHsaEG5014776	132
FMOD	Fibromodulin	dHsaEG5014378	114
SMAD2	SMAD family member 2	dHsaEG5024257	115
TGFBR1	Transforming growth factor beta receptor 1	dHsaEG5016420	91
TGFBR3	Transforming growth factor beta receptor 3	dHsaEG5016301	102
TJP1	Tight junction protein 1	dHsaEG5022982	142
GAPDH[a]	Glyceraldehyde-3-phosphate dehydrogenase	dHsaEG5006642	117
HPRT1[a]	Hypoxanthine phosphoribosyltransferase 1	dHsaEG5189658	90

[a]These two assays are reference genes used in expression profiling of stretched primary human SC endothelial cells.

Table 3. Primers Designed for Real-Time PCR to Examine Gene Expression in Bovine AAP Endothelial Cells

Gene Symbol	Gene Description	Primers (F)	Primers (R)
CDH2	N-cadherin	CGAGCCAGCAGATTTTAAGG	GATGGGAGGGATAACCCAGT
CDH6	K-cadherin	CCACTGTTCCCGAAATGTCT	CGTGATGTTCACCGTGGTAG
CDH11	OB-cadherin	AGACCAAGCCACATTCCAAC	ATTCACGTCACACCCACAGA
SMAD2	SMAD family member 2	ATGGTCGTCTTCAGGTGTCC	GCAGTTCCGTTAGGATCTCG
CAV1	Caveolin 1	AGCCCAACAACAAGGCTATG	GATGCCATCGAAACTGTGTG
CAV2	Caveolin 2	ATCTGCAGCCACGCTCTATT	CTGCGTCCTATGCTCGTACA
TGFBR1	Transforming growth factor beta receptor 1	CTCAGCTCTGGTTGGTGTCA	CACTCTGTGGTTTGGAGCAA
GAS7	Growth arrest-specific 7	GGCTGGCAAAGCTACTTGTC	TGGAATCCCAGAAGAACTGC
CYP1B1	Cytochrome P450, family 1, subfamily B, member 1	CACGGTCACAGACATCTTCG	GTGCCTACCCACCACTTGAT
ABCA1	ATP binding cassette subfamily A member 1	TCGCTTACTTGCAGGATGTG	TGCTGATGAACCAGCTGAAC
FMOD	Fibromodulin	CCTGGCCTCAAATACCTTCA	CACCTGCAGCTTGGAGAAGT
BMP4	Bone morphogenetic protein 4	AGTCTGGGGAGGAGGAAGAG	TACGATGAAAGCCCTGATCC
OCLN	Occludin	ATGGGAGTCAATCCAACTGC	CGTTCCTTGTCCCACAGAAT
TJP2	Tight junction protein 2	GCAGTCTGGGTCTCTGAAGG	GCTCATCCAGCTCATTGTCA
CLDN11	Claudin 11	CTGGTGGACATCCTCATCCT	GCGTACAGGGAGTAGCCAAA
GAPDH[a]	Glyceraldehyde-3-phosphate dehydrogenase	GGGTCATCATCTCTGCACCT	GGTCATAAGTCCCTCCACGA
HPRT1[a]	Hypoxanthine phosphoribosyltransferase 1	GCCGACCTGTTGGATTACAT	ACACTTCGAGGGGTCCTTTT

[a]These two pairs of primers are reference genes used in expression profiling of bovine AAP cells.

Corning, NY), followed by seeding into a 2% gelatin-coated T25 flask. The isolated cells were allowed to reach 90% to 100% confluence, with medium changes every 2 days (up to 10 days).[28]

Selection of AAP Cells by Puromycin Treatment

When the isolated outflow cells reached confluence, the culture medium was replaced with complete medium containing 4-µg/mL puromycin for 2 days, according to an established protocol used for porcine outflow cells.[28] The medium was then aspirated and cells were washed with phosphate-buffered saline (PBS) twice to remove dead cells. The medium was changed to complete culture medium for cell repopulation.

Immunofluorescence Staining of Cells

The cells were seeded onto 2% gelatin-coated coverslips in six-well plates. After reaching confluence, cells were fixed with 4% formaldehyde for 15 minutes and washed with PBS three times. The cells were then blocked in 5% bovine serum albumin (BSA) (Sigma-

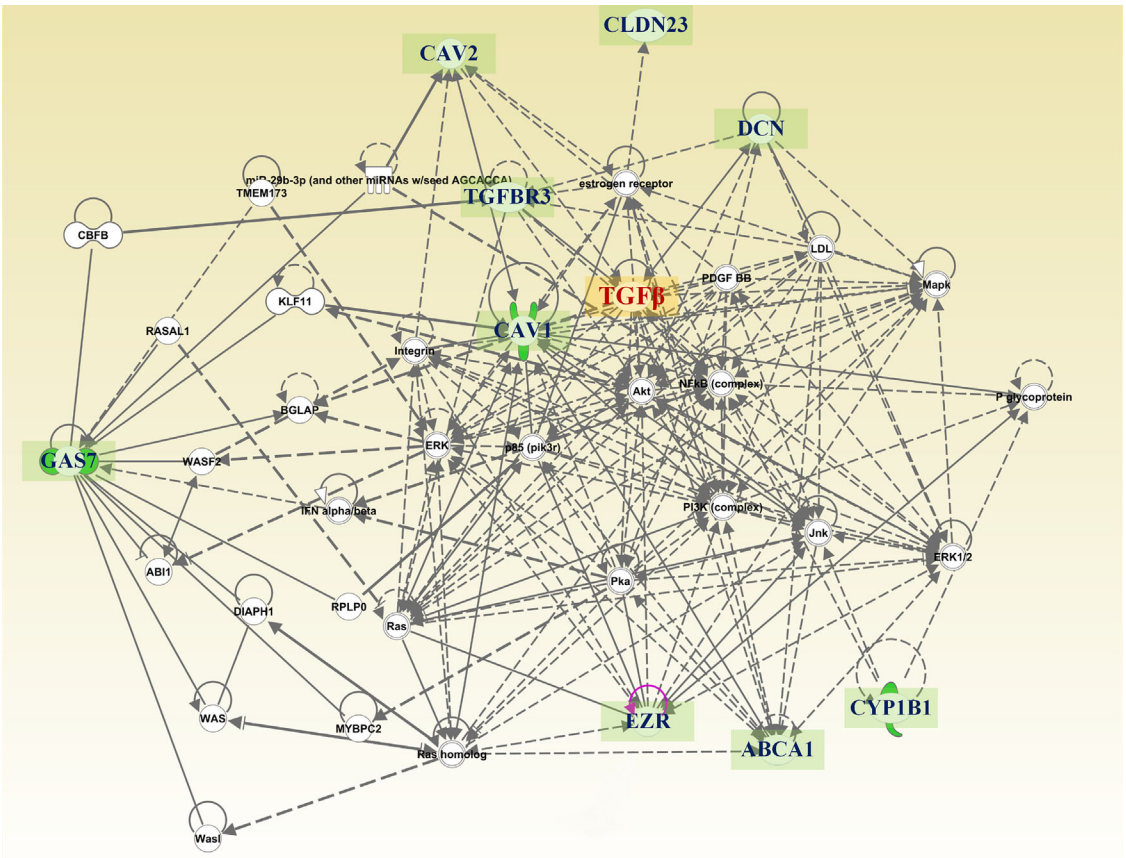

Figure 2. Merged network of differentially expressed genes according to annotated information in the IPA database. The genes of interest are magnified and bolded. These genes are connected, directly (*solid line*) or indirectly (*dotted line*), to TGFβ pathways in the network shown here. *Arrows* point toward the object of regulation.

Table 4. Differentially Expressed Genes in Mechanically Stretched Primary Human SC Endothelial Cells

Gene	Description	Fold Change (Stretch)	*P*	TGFβ Relation
ABCA1	ATP binding cassette subfamily A member 1	1.65	0.02	ERK1/2, JNK
CAV2	Caveolin 2	1.25	0.044	JNK
CLDN23	Claudin 23	1.43	0.029	Indirect
CYP1B1	Cytochrome P450, family 1, subfamily B, member 1	1.44	0.05	JNK
DCN	Decorin	1.74	0.001	Direct
EZR	Ezrin	1.44	0.013	ERK
FMOD	Fibromodulin	1.57	0.048	Direct
GAS7	Growth arrest-specific 7	1.81	0.02	Indirect
TGFBR3	Transforming growth factor beta receptor 3	1.33	0.019	Direct

Aldrich) for 1 hour at room temperature and permeabilized with 0.2% Triton X-100 (Sigma-Aldrich) for 5 minutes. Cells were incubated with 5% BSA (negative control), antibodies against Von Willebrand factor (VWF) (Abcam6994, 1:400; Abcam, Cambridge, UK), or VE-cadherin (Abcam232880, 1:200) overnight at 4°C. Cells were washed with PBS three times and incubated with Alexa Fluor 488 Goat anti-Rabbit Secondary Antibody (Thermo Fisher Scientific) at room temperature for 30 minutes before mounting with ProLong Diamond Antifade Mountant and 4′,6-diamidino-2-phenylindole (Thermo Fisher Scientific). Five images were taken from randomly selected sections of cells grown on a coverslip using an immunofluorescence microscope (HBO 100; Carl Zeiss Meditec, Oberkochen, Germany)

Table 5. Genes Examined in the SC and AAP Cells Under TGFβ2 Treatment

Gene	Description	Functional Category
TGFBR1	Transforming growth factor beta receptor 1	TGFβ binding
SMAD2	SMAD family member 2	TGFβ binding
BMP4	Bone morphogenetic protein 4	TGFβ binding
CYP1B1	Cytochrome P450, family 1, subfamily B, member 1	Oxidoreductase activity
DCN	Decorin	Collagen binding
EZR	Ezrin	Actin filament binding
GAS7	Growth arrest-specific 7	Actin filament binding
CDH2	Cadherin 2	Cell–cell adhesion
TJP1	Tight junction protein 1	Cell–cell adhesion

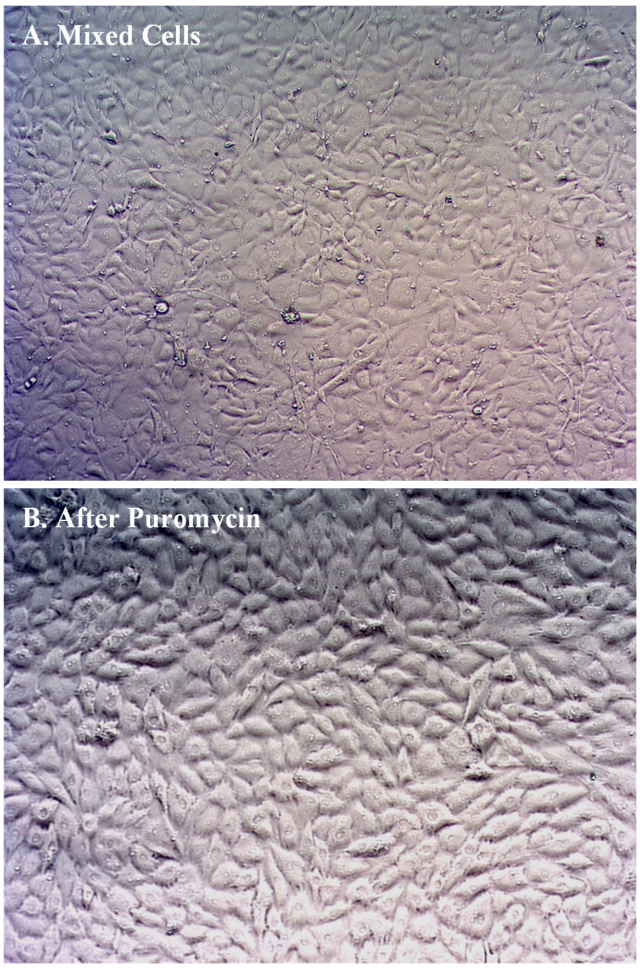

Figure 3. Phase-contrast microscopy of cultured bovine ocular cells from outflow tissues. (A) Prior to puromycin treatment, the different types of cells grew overlapped in the flask. (B) After exposure to puromycin, the remaining cells repopulated and displayed relatively uniform morphology.

to calculate the purity of culture by dividing the VWF-positive cells of nuclei counts as previously described.[28]

Transforming Growth Factor Beta-2 Treatment with Bovine AAP Cells and Human SC Cells

AAP and SC cells were cultured in six-well plates with duplicates from each batch or each strain. After reaching 80% confluence, three batches of primary bovine AAP cells or three strains of primary human SC cells were treated with or without recombinant human transforming growth factor beta-2 (TGFβ2) protein (Abcam) at 5 ng/mL and 10 ng/mL in fetal bovine serum-free culture medium for 24 or 48 hours. Total RNA was then isolated using Invitrogen TRIzol (Thermo Fisher Scientific) according to the manufacturer's recommended protocol for further gene expression profiling.[31] For consistent expression profiling, we examined the gene expression response of TGFβ2 treatment in SC cells using Bio-Rad ddPCR assays as previously described.[30,32–37] All of the ddPCR assays are listed in Table 2.

Expression Profiling in Bovine AAP Cells Using Real-Time PCR

The mRNA sequences for bovine genes were obtained from the cow genome sequence data bosTau8 on the University of California, Santa Cruz, genome website (https://genome.ucsc.edu/cgi-bin/hgGateway). Because there are no available predesigned and in silico validated ddPCR assays for bovine genes from Bio-Rad, we used Primer3 (http://primer3.ut.ee/) to design specific primers for these targeted genes (Table 3). The PCR amplicons were designed to span intron–exon boundaries to eliminate potential DNA contamination. Real-time PCR was performed using the Bio-Rad SYBR Green Supermix and an Applied Biosystems StepOne Real-Time PCR System (Thermo Fisher Scientific). *GAPDH* was used as an internal reference gene after comparison with other housekeeping genes, including *HPRT1, RPLP0,* and *ACTB*.

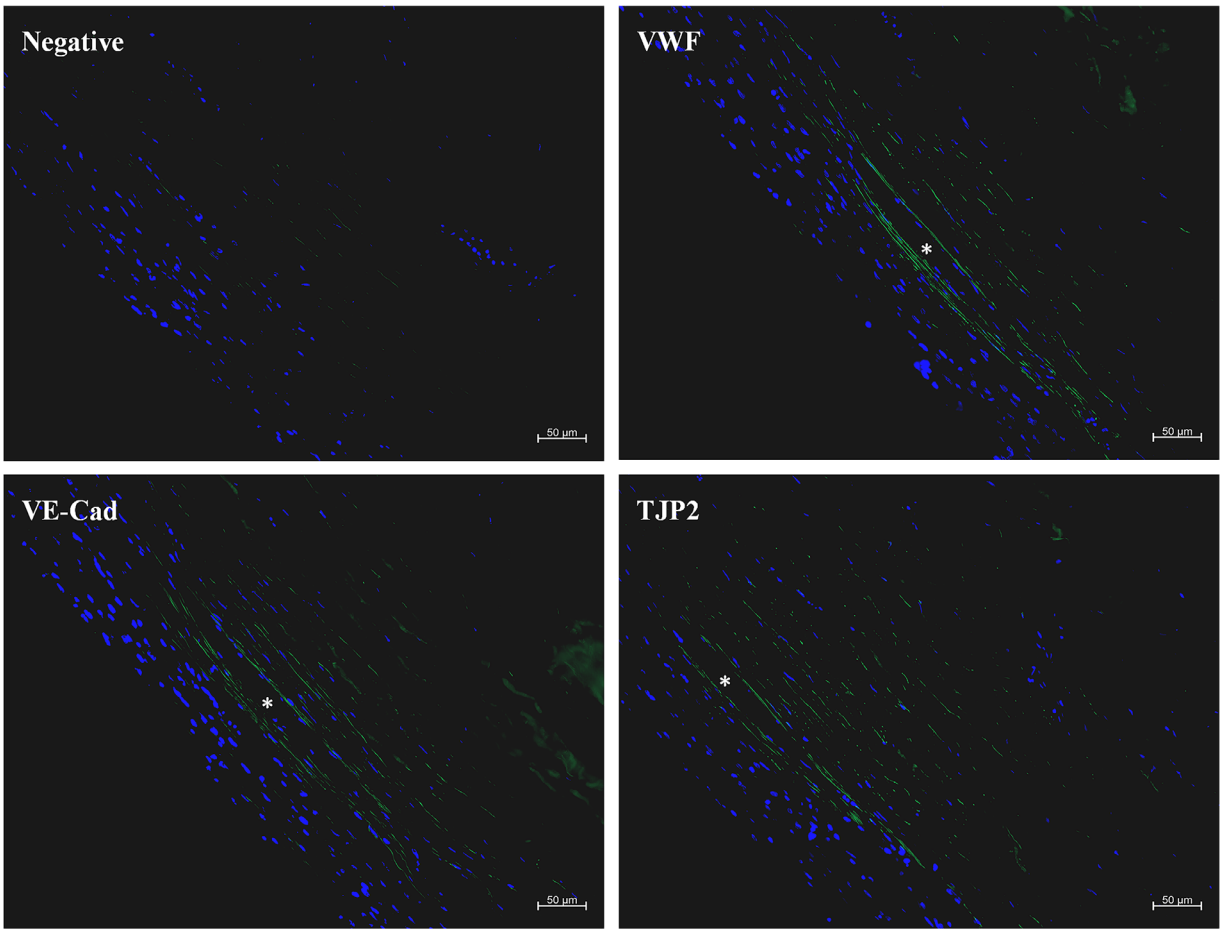

Figure 4. Expression of three endothelial marker proteins in stained sections of the TM region containing AAP visualized by immunofluorescence microscopy. The immunofluorescence images show the expression of vWF, VE-cadherin, and tight junction protein 2 (TJP2) by AAP cells. The endothelial marker proteins are shown in *green*, and nuclei are shown in *blue*. Asterisk shows location of aqueous plexus lumen. *Scale bar*: 50 µm.

Statistical Analysis

Results from the technical duplicates were averaged prior to statistical analysis. Data were analyzed using the Student's *t*-test with Bonferroni–Dunn correction performed in Prism 8.02 (GraphPad, San Diego, CA) with statistical significance set at $P \leq 0.05$.

Results

Expression of Glaucoma-Related Genes in Stretched SC Cells

To identify glaucoma-related genes that are responsive to mechanical strain, the genes that were found to be differentially expressed in glaucoma SC cells were profiled in stretched SC cells in comparison with non-stretched SC cells (n = 3).[30] The ddPCR results showed that nine glaucoma-related genes were significantly induced with mechanical strain (Table 4). The identified glaucoma-associated genes *ABCA1, CAV2, CYP1B1,* and *GAS7* were induced by stretch, suggesting their potential role in the biomechanical function of SC cells.[38] The extracellular matrix (ECM) genes *DCN,*, *EZR,* and *FMOD* showed significant alterations after stretch, corresponding to the ECM turnover in stretched cells.[39]

Ingenuity Pathway Analysis

To determine the connections and potential regulators of these mechanoresponsive glaucoma-related genes, we performed pathway analysis and upstream regulator analysis using IPA software. Both analyses identified a key factor, TGFβ, which was associated with almost all genes of interest. Additionally, several connectors were revealed with the merged network generation of these mechanoresponsive genes, and TGFβ was found prominently at one of the nodes

(Fig. 2). *ABCA1* and *CYP1B1* were related through the non-canonical pathways by c-Jun N-terminal kinase (JNK) or extracellular signal-regulated kinases 1 and 2 (ERK1/2), whereas *CAV2, TGFBR3,* and *DCN* were directly related to TGFβ regulation (Table 4). In addition, fibromodulin (FMOD) is a known modulator of TGFβ.[40] Because the association of TGFβ as an upstream regulator was highly significant ($P = 2.33 \times 10^{-6}$) and all differentially expressed genes were engaged in the TGFβ pathway, we decided to further study the role of TGFβ on these mechanoresponsive glaucoma-related genes in bovine AAP cells first, followed by validation in human SC cells.

Puromycin Selection of AAP Cells

Primary cells cultured from bovine outflow tissues had a mixture of cell types with a variety of morphologies, including overlapping growth. After puromycin treatment, approximately two-thirds of the cells died, and the remaining cells repopulated to confluence in approximate 10 days. The confluent puromycin-selected cells formed a cobblestone-like monolayer with polygonal morphology and contact inhibition, which are characteristic features of endothelial cells that distinguish AAP cells from trabecular meshwork cells (Fig. 3). The immunofluorescent staining of intact bovine anterior chamber sections demonstrated specific expression of endothelial marker proteins in AAP cells, such as VWF, VE-cadherin, and tight junction protein 2 (TJP2) (Fig. 4). All of the puromycin-selected cells expressed the endothelial marker proteins VWF and VE-cadherin (Fig. 5), suggesting a successful selection and pure AAP culture.

TGFβ2 Treatment on AAP and SC Cells

Due to the variation between human and bovine genomes, bovine cells do not express several glaucoma-related genes found in humans, such as *TGFBR3* and *CLDN23*. Therefore, we focused our investigation on three groups of functional genes related to TGFβ2 treatment, including TGFβ signaling pathway genes, glaucoma-related genes identified in stretched human SC cells, and cell adhesion genes related to the permeability of AAP cells (Table 5). We treated three batches of AAP cells and three strains of primary human SC cells with different concentrations of TGFβ2 at two time points to monitor changes in expression.

The TGFβ SMAD signaling pathway was activated and *BMP4* was downregulated (Fig. 6). We also found that four of the mechanoresponsive glaucoma-related genes responded to TGFβ2 treatment; for example, *CYP1B1* and *DCN* were inhibited but *EZR* was

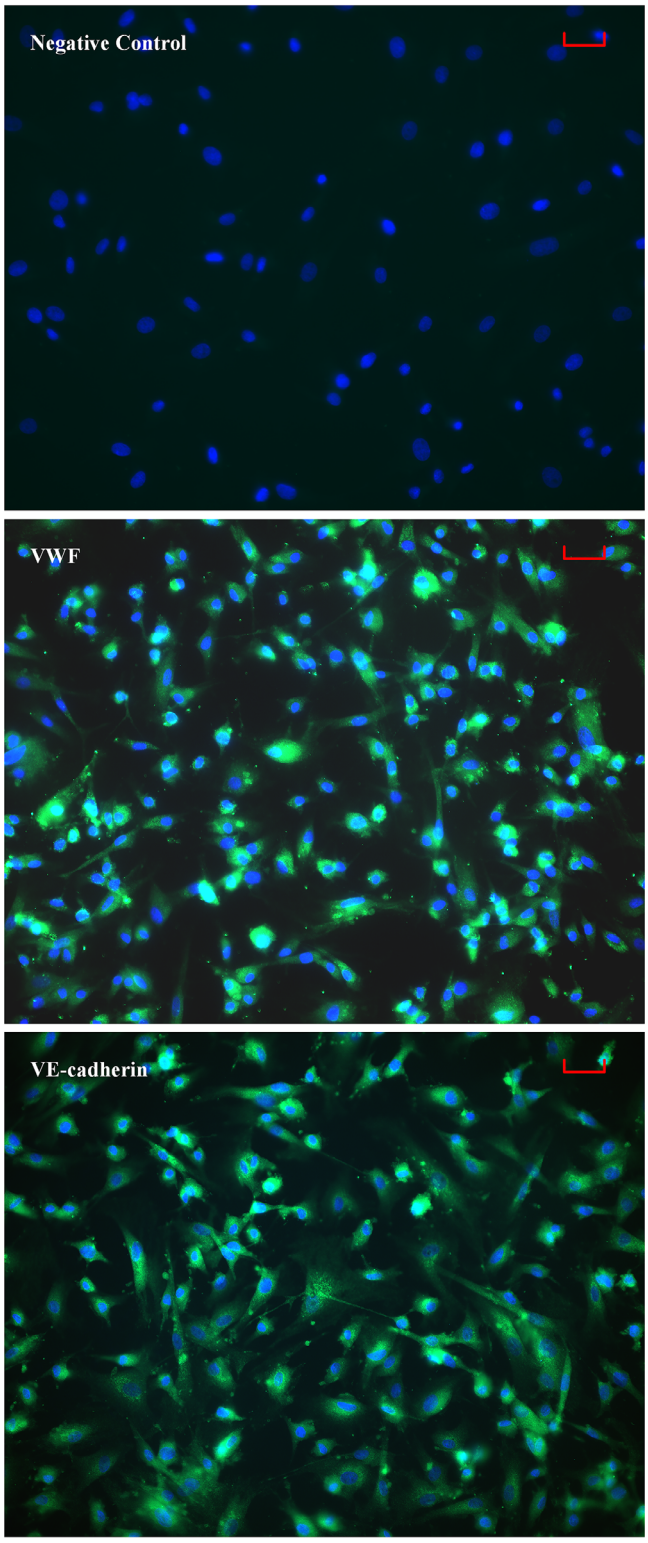

Figure 5. Expression of two endothelial marker proteins in puromycin-treated cells. The cells expressed typical endothelial markers vWF and VE-cadherin. All images are shown with the same magnification (20×). *Scale bar*: 50 µm.

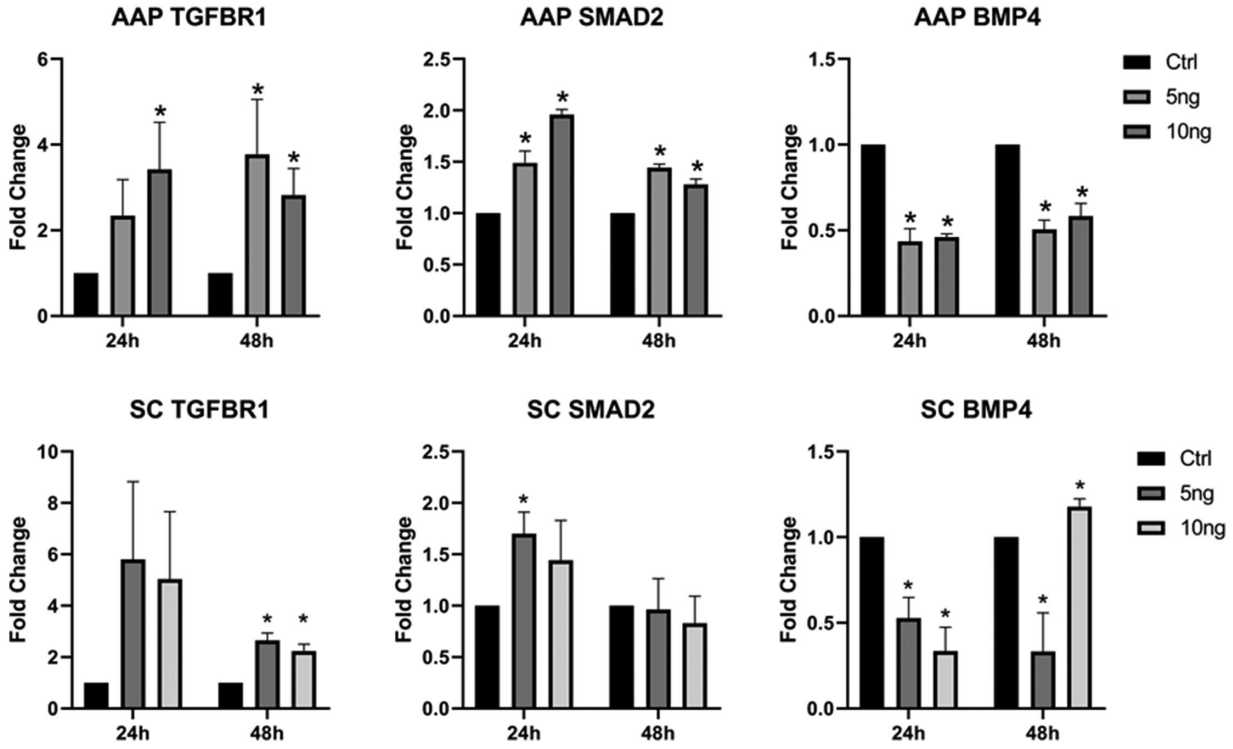

Figure 6. Differential expression of TGFβ signaling pathway genes following TGFβ2 treatment in primary bovine AAP cells (n = 3) and human SC cells (n = 3). The expression level of the control group was set as 1.0-fold, and each treatment group was compared to corresponding control group with the same observation time. $^{*}P < 0.05$; error bars, standard deviation.

induced in both AAP and SC cells. Although *GAS7* showed different alterations between the two cell types, it responded significantly to the treatment in both. The effect was dependent on time and concentration, especially in human SC cells (Fig. 7). Because cell–cell adhesion between endothelial cells is one of the crucial characteristics to maintain integrity and function of SC endothelium, we examined the differential expression of these genes after TGFβ2 treatment. The mRNA expression of *TJP2* or *TJP1* had no significant increase after treatment; however, the cell–cell adhesion gene *CDH2* (N-cadherin) was significantly induced (Fig. 8).

Discussion

We successfully isolated, characterized, and cultured endothelial cells from bovine AAP. The integrated analysis of glaucoma genetics and mechanoresponsive genes of human SC cells led to investigation of the TGFβ2 effect on our new cell model for human SC. We observed that bovine AAP and human SC cells responded similarly to TGFβ2 treatment, validating the usage of bovine AAP cells to study human SC cell biology.

Previously, we found differentially expressed genes in SC cells isolated from glaucomatous donor eyes,[30] but the function of these genes in SC cells remains unclear. Because biomechanical strain is a trigger for pore formation in cultured human SC cells, we examined the differentially expressed genes in stretched SC cells.[11] Interestingly, the glaucoma-related genes were induced in normal SC cells after mechanical stretch, whereas they were mostly downregulated in glaucomatous SC cells.[30] These differences indicate the potential dysfunction of the mechanoresponsive pathways in glaucomatous SC cells, leading to fewer pore openings and a significant resistance that increases IOP.

Our pathway analysis of mechanoresponsive genes revealed TGFβ to be a common upstream regulator. Significantly, many previous studies have reported an increased level of TGFβ2 in aqueous humor of glaucomatous eyes.[41] Moreover, perfusing TGFβ2 into human eyes leads to the accumulation of fibrillary ECM under the inner wall of SC and increased outflow resistance.[42] Although the TGFβ2 effects on TM cells have been studied extensively,[43–45] this is the first study, to our knowledge, to report the effect of TGFβ2 on SC and AAP cells.

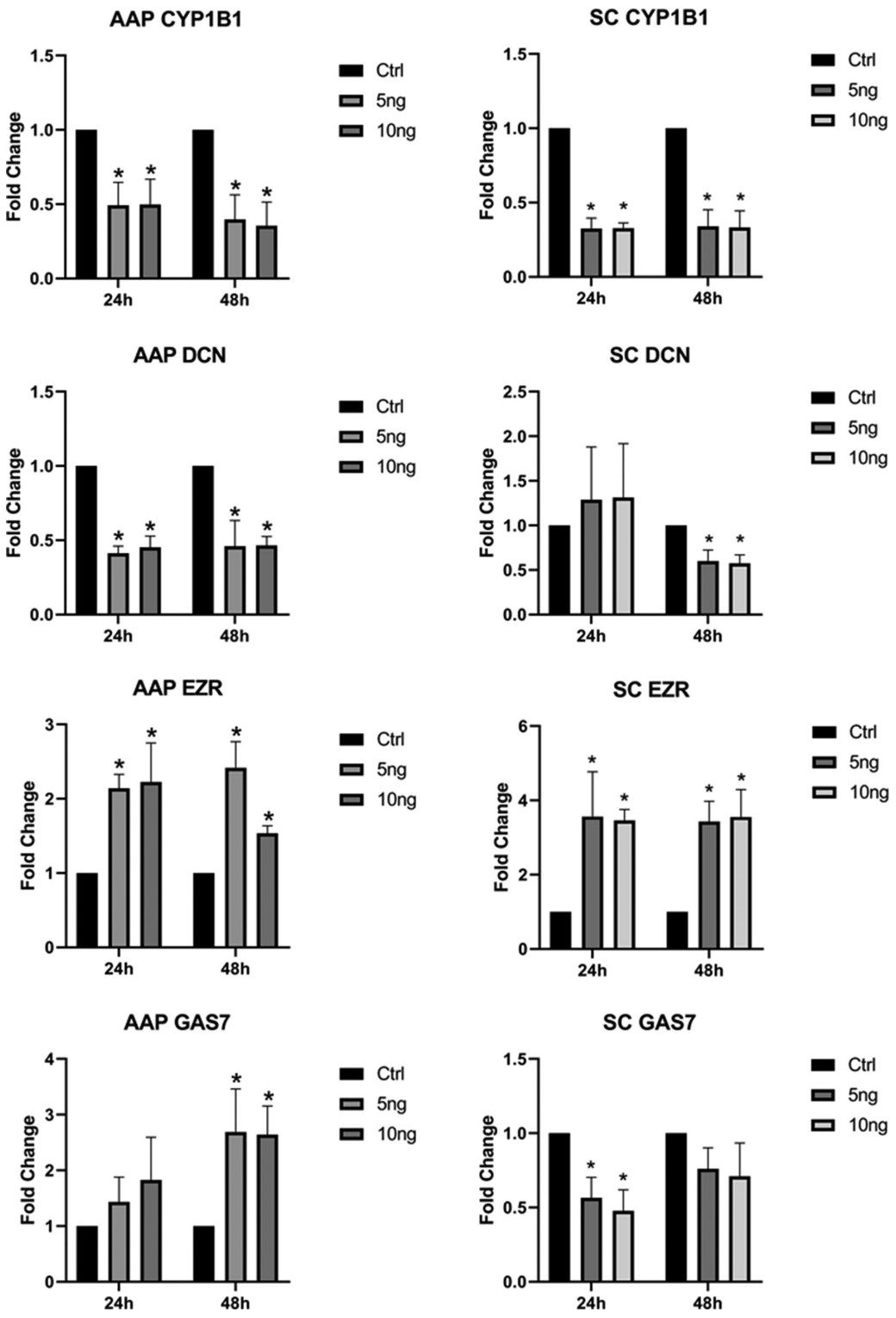

Figure 7. Differential expression of glaucoma-related genes following TGFβ2 treatment in primary bovine AAP cells (n = 3) and human SC cells (n = 3). $^{*}P < 0.05$; error bars, standard deviation.

TGFβ2 can activate a large number of signaling pathways,[46] which may be related to fibrosis and tissue stiffening as observed in glaucomatous eyes.[47–49] Based on the results from previous studies using TM cells, we examined activation of the canonical signaling pathway through the TGFβ receptor and BMP ligands.[50] Thus, *TGFBR1* expression was activated and *BMP4* expression was suppressed. The activation of *SMAD2*

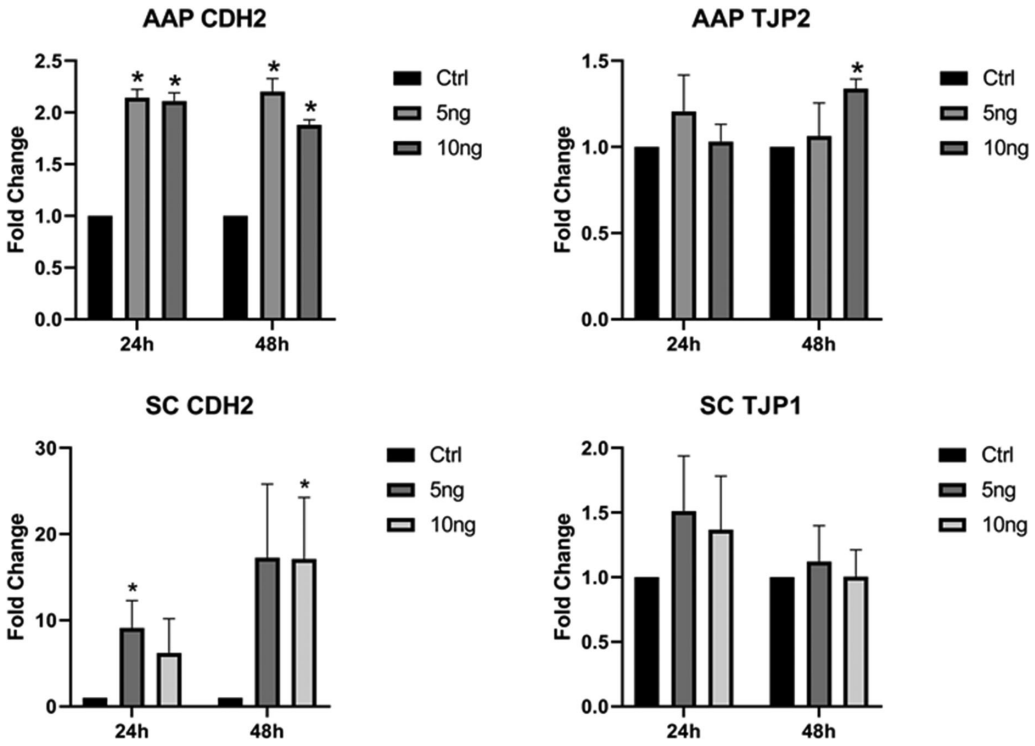

Figure 8. Differential expression of cell adhesion genes following TGFβ2 treatment of primary bovine AAP cells (n = 3) and human SC cells (n = 3). $^{*}P < 0.05$; error bars, standard deviation.

decreased over long-term treatment, indicating an early response to TGFβ2 treatment. We then examined the expression of glaucoma-related genes that were also mechanoresponsive. Interestingly, TGFβ2 inhibited the mechanoresponsive genes in SC cells, coincident with the dysfunction of these genes in glaucomatous SC cells.[30] Finally, it is known that TGFβ promotes cell adhesion and tight junction assembly, which are integral for pore formation in the SC inner wall.[13,51,52] We found that N-cadherin (*CDH2*) was significantly induced, but not tight junction protein (*TJP1*). The small effect on tight junction expression may be due to the subconfluence (80%) of cells at the beginning of TGFβ2 treatment.

The limited source of SC cells has interfered with progress in the study of SC cell biology. We were thus motivated to develop a "workhorse" in vitro cellular model for human SC cells. Bovine eyes are commonly used in the study of conventional outflow biology.[53,54] For example, glucocorticoid treatment of bovine eyes induces ECM accumulation in the TM region containing AAP and causes ocular hypertension, similar to that seen in human eyes.[55] Additionally, bovine TM cells have been a reliable and translatable model to human TM cells.[56,57] However, the isolation of bovine AAP cells has been impeded by the tortuous AAP loops and small number of cells in each eye. Here, we demonstrate that the puromycin selection technique is a convenient method for purifying AAP cells from a mixed culture of bovine outflow cells. Our selected cells were validated by histological location, cobblestone-like morphology, contact inhibition, and standard endothelial markers. The TGFβ signaling pathway activation and glaucoma-related genes responded similarly to TGFβ2 treatment in human SC cells, supporting the usage of AAP cells as an alternative cellular model of SC cells.

The bovine cellular model also had limitations. First, due to the species variation, bovine cells express different types of proteins in comparison to humans; for example, bovine cells express TJP2/ZO-2 rather than TJP1/ZO-1, which is expressed in human cells. Second, the bovine donors are less than 1 to 2 years old, equivalent to teenage humans, which are younger than most human donors. The age difference likely contributes to the response diversity between these two models. The different responses of *GAS7* between human and bovine cells may be attributed to either species or age variation. Third, with fewer variations in genetic background, the AAP cellular model generates a relatively more uniform response to treatment than human SC cells. *DCN* expression was suppressed in all strains of AAP cells, whereas three strains of human SC cells had distinct

expressions of *DCN* with 24 hours of treatment. Therefore, the AAP cell appears to be a good model for initial studies, which can be later validated in human SC cells.

In summary, we identified glaucoma-related genes in human SC cells that robustly responded to a relevant mechanical stimulus. Significantly, these genes also respond to TGFβ2 treatment in SC cells, matching a pattern of gene expression previously observed in glaucomatous SC cells and supporting a vital role for TGFβ2 in glaucoma development. We observed a very similar pattern of gene expression changes in our novel and fully characterized bovine AAP cell model after TGFβ2 treatment. As in the TM, our data implicate TGFβ2 as a key player in glaucomatous changes in SC and support the utility of our bovine AAP cellular model in studying SC biology.

Acknowledgments

The authors thank all of the donors for their gift of ocular samples for the research.

Supported by Grants from The Glaucoma Foundation, The Glaucoma Research Foundation, The BrightFocus Foundation, NIH R01EY023242, R21EY028671, R01EY022359, R01EY028608, R01EY019696, P30EY03631, and P30EY005722. None of the funding sources has influenced the experimental design, data generation, or analysis.

This manuscript was presented at the ISER/BrightFocus 2019 Glaucoma Symposium in Atlanta, GA, by J Cai.

Disclosure: **J. Cai**, None; **K. Perkumas**, None; **W.D. Stamer**, None; **Y. Liu**, None

References

1. Tham YC, Li X, Wong TY, Quigley HA, Aung T, Cheng CY. Global prevalence of glaucoma and projections of glaucoma burden through 2040: a systematic review and meta-analysis. *Ophthalmology*. 2014;121:2081–2090.
2. Kingman S. Glaucoma is second leading cause of blindness globally. *Bull World Health Organ*. 2004;82:887–888.
3. Jonas JB, Aung T, Bourne RR, Bron AM, Ritch R, Panda-Jonas S. Glaucoma. *Lancet*. 2017;390:2183–2193.
4. Ethier CR, Coloma FM, de Kater AW, Allingham RR. Retroperfusion studies of the aqueous outflow system. Part 2: Studies in human eyes. *Invest Ophthalmol Vis Sci*. 1995;36:2466–2475.
5. Stamer WD, Acott TS. Current understanding of conventional outflow dysfunction in glaucoma. *Curr Opin Ophthalmol*. 2012;23:135–143.
6. Last JA, Pan T, Ding Y, et al. Elastic modulus determination of normal and glaucomatous human trabecular meshwork. *Invest Ophthalmol Vis Sci*. 2011;52:2147–2152.
7. Overby DR, Zhou EH, Vargas-Pinto R, et al. Altered mechanobiology of Schlemm's canal endothelial cells in glaucoma. *Proc Natl Acad Sci USA*. 2014;111:13876–13881.
8. Vahabikashi A, Gelman A, Dong B, et al. Increased stiffness and flow resistance of the inner wall of Schlemm's canal in glaucomatous human eyes. *Proc Natl Acad Sci USA*. 2019;116:26555–26563.
9. Stamer WD, Braakman ST, Zhou EH, et al. Biomechanics of Schlemm's canal endothelium and intraocular pressure reduction. *Prog Retin Eye Res*. 2015;44:86–98.
10. Michel CC, Neal CR. Openings through endothelial cells associated with increased microvascular permeability. *Microcirculation*. 1999;6:45–54.
11. Braakman ST, Pedrigi RM, Read AT, et al. Biomechanical strain as a trigger for pore formation in Schlemm's canal endothelial cells. *Exp Eye Res*. 2014;127:224–235.
12. Allingham RR, Damji KF, Freedman SF, Moroi SE, Rhee DJ, Shields B. *Shields Textbook of Glaucoma*. 6th ed. Philadelphia, PA: Lippincott Williams & Wilkins; 2011.
13. Ethier CR. The inner wall of Schlemm's canal. *Exp Eye Res*. 2002;74:161–172.
14. Stamer WD, Roberts BC, Howell DN, Epstein DL. Isolation, culture, and characterization of endothelial cells from Schlemm's canal. *Invest Ophthalmol Vis Sci*. 1998;39:1804–1812.
15. Alvarado JA, Betanzos A, Franse-Carman L, Chen J, Gonzalez-Mariscal L. Endothelia of Schlemm's canal and trabecular meshwork: distinct molecular, functional, and anatomic features. *Am J Physiol Cell Physiol*. 2004;286:C621–C634.
16. Karl MO, Fleischhauer JC, Stamer WD, et al. Differential P1-purinergic modulation of human Schlemm's canal inner-wall cells. *Am J Physiol Cell Physiol*. 2005;288:C784–C794.
17. Curcio CA, Research Tissue Acquisition Working Group. Declining availability of human eye tissues for research. *Invest Ophthalmol Vis Sci*. 2006;47:2747–2749.

18. Bouhenni RA, Dunmire J, Sewell A, Edward DP. Animal models of glaucoma. *J Biomed Biotechnol*. 2012;2012:692609.
19. Johnson TV, Tomarev SI. Rodent models of glaucoma. *Brain Res Bull*. 2010;81:349–358.
20. McMenamin PG, Steptoe RJ. Normal anatomy of the aqueous humour outflow system in the domestic pig eye. *J Anat*. 1991;178:65–77.
21. Pizzirani S, Gong H. Functional anatomy of the outflow facilities. *Vet Clin N Am Small Anim Pract*. 2015;45:1101–1126.
22. Mao W, Tovar-Vidales T, Yorio T, Wordinger RJ, Clark AF. Perfusion-cultured bovine anterior segments as an ex vivo model for studying glucocorticoid-induced ocular hypertension and glaucoma. *Invest Ophthalmol Vis Sci*. 2011;52:8068–8075.
23. Overby D, Gong H, Qiu G, Freddo TF, Johnson M. The mechanism of increasing outflow facility during washout in the bovine eye. *Invest Ophthalmol Vis Sci*. 2002;43:3455–3464.
24. Loewen RT, Roy P, Park DB, et al. A porcine anterior segment perfusion and transduction model with direct visualization of the trabecular meshwork. *Invest Ophthalmol Vis Sci*. 2016;57:1338–1344.
25. Bhatt K, Gong H, Freddo TF. Freeze-fracture studies of interendothelial junctions in the angle of the human eye. *Invest Ophthalmol Vis Sci*. 1995;36:1379–1389.
26. Tripathi RC, Tripathi BJ. The mechanism of aqueous outflow in lower mammals. *Exp Eye Res*. 1972;14:73–79.
27. Ramos RF, Hoying JB, Witte MH, Daniel Stamer W. Schlemm's canal endothelia, lymphatic, or blood vasculature? *J Glaucoma*. 2007;16:391–405.
28. Lei Y, Overby DR, Read AT, Stamer WD, Ethier CR. A new method for selection of angular aqueous plexus cells from porcine eyes: a model for Schlemm's canal endothelium. *Invest Ophthalmol Vis Sci*. 2010;51:5744–5750.
29. Perkumas KM, Stamer WD. Protein markers and differentiation in culture for Schlemm's canal endothelial cells. *Exp Eye Res*. 2012;96:82–87.
30. Cai J, Perkumas KM, Qin X, Hauser MA, Stamer WD, Liu Y. Expression profiling of human Schlemm's canal endothelial cells from eyes with and without glaucoma. *Invest Ophthalmol Vis Sci*. 2015;56:6747–6753.
31. Rio DC, Ares M Jr, Hannon GJ, Nilsen TW. Purification of RNA using TRIzol (TRI reagent). *Cold Spring Harbor Protoc*. 2010;2010:pdb.prot5439.
32. Youngblood H, Cai J, Drewry MD, et al. Expression of mRNAs, miRNAs, and lncRNAs in human trabecular meshwork cells upon mechanical stretch. *Invest Ophthalmol Vis Sci*. 2020;61:2.
33. Khaled ML, Bykhovskaya Y, Gu C, et al. PPIP5K2 and PCSK1 are candidate genetic contributors to familial keratoconus. *Sci Rep*. 2019;9:19406.
34. Khaled ML, Bykhovskaya Y, Yablonski SER, et al. Differential expression of coding and long noncoding RNAs in keratoconus-affected corneas. *Invest Ophthalmol Vis Sci*. 2018;59:2717–2728.
35. Helwa I, Cai J, Drewry MD, et al. A comparative study of serum exosome isolation using differential ultracentrifugation and three commercial reagents. *PLoS One*. 2017;12:e0170628.
36. Liu Y, Bailey JC, Helwa I, et al. A common variant in MIR182 is associated with primary open-angle glaucoma in the NEIGHBORHOOD consortium. *Invest Ophthalmol Vis Sci*. 2016;57:4528–4535.
37. Drewry M, Helwa I, Allingham RR, Hauser MA, Liu Y. miRNA profile in three different normal human ocular tissues by miRNA-Seq. *Invest Ophthalmol Vis Sci*. 2016;57:3731–3739.
38. Liu Y, Allingham RR. Major review: molecular genetics of primary open-angle glaucoma. *Exp Eye Res*. 2017;160:62–84.
39. Bradley JM, Kelley MJ, Zhu X, Anderssohn AM, Alexander JP, Acott TS. Effects of mechanical stretching on trabecular matrix metalloproteinases. *Invest Ophthalmol Vis Sci*. 2001;42:1505–1513.
40. Soo C, Hu FY, Zhang X, et al. Differential expression of fibromodulin, a transforming growth factor-beta modulator, in fetal skin development and scarless repair. *Am J Pathol*. 2000;157:423–433.
41. Prendes MA, Harris A, Wirostko BM, Gerber AL, Siesky B. The role of transforming growth factor beta in glaucoma and the therapeutic implications. *Br J Ophthalmol*. 2013;97:680–686.
42. Gottanka J, Chan D, Eichhorn M, Lutjen-Drecoll E, Ethier CR. Effects of TGF-beta2 in perfused human eyes. *Invest Ophthalmol Vis Sci*. 2004;45:153–158.
43. Fuchshofer R, Stephan DA, Russell P, Tamm ER. Gene expression profiling of TGFbeta2- and/or BMP7-treated trabecular meshwork cells: identification of Smad7 as a critical inhibitor of TGF-beta2 signaling. *Exp Eye Res*. 2009;88:1020–1032.
44. Fleenor DL, Shepard AR, Hellberg PE, Jacobson N, Pang IH, Clark AF. TGFbeta2-induced changes in human trabecular meshwork: implications for intraocular pressure. *Invest Ophthalmol Vis Sci*. 2006;47:226–234.

45. Wordinger RJ, Fleenor DL, Hellberg PE, et al. Effects of TGF-beta2, BMP-4, and gremlin in the trabecular meshwork: implications for glaucoma. *Invest Ophthalmol Vis Sci*. 2007;48:1191–1200.
46. Ikushima H, Miyazono K. Biology of transforming growth factor-β signaling. *Curr Pharm Biotechnol*. 2011;12:2099–2107.
47. Robertson JV, Golesic E, Gauldie J, West-Mays JA. Ocular gene transfer of active TGF-beta induces changes in anterior segment morphology and elevated IOP in rats. *Invest Ophthalmol Vis Sci*. 2010;51:308–318.
48. Zhavoronkov A, Izumchenko E, Kanherkar RR, et al. Pro-fibrotic pathway activation in trabecular meshwork and lamina cribrosa is the main driving force of glaucoma. *Cell Cycle*. 2016;15:1643–1652.
49. Coudrillier B, Pijanka JK, Jefferys JL, et al. Glaucoma-related changes in the mechanical properties and collagen micro-architecture of the human sclera. *PLoS One*. 2015;10:e0131396.
50. Wordinger RJ, Sharma T, Clark AF. The role of TGF-beta2 and bone morphogenetic proteins in the trabecular meshwork and glaucoma. *J Ocul Pharmacol Ther*. 2014;30:154–162.
51. Wang H, Radjendirane V, Wary KK, Chakrabarty S. Transforming growth factor beta regulates cell-cell adhesion through extracellular matrix remodeling and activation of focal adhesion kinase in human colon carcinoma Moser cells. *Oncogene*. 2004;23:5558–5561.
52. Howe KL, Reardon C, Wang A, Nazli A, McKay DM. Transforming growth factor-beta regulation of epithelial tight junction proteins enhances barrier function and blocks enterohemorrhagic *Escherichia coli* O157:H7-induced increased permeability. *Am J Pathol*. 2005;167:1587–1597.
53. Wiederholt M, Bielka S, Schweig F, Lutjen-Drecoll E, Lepple-Wienhues A. Regulation of outflow rate and resistance in the perfused anterior segment of the bovine eye. *Exp Eye Res*. 1995;61:223–234.
54. Lu Z, Overby DR, Scott PA, Freddo TF, Gong H. The mechanism of increasing outflow facility by rho-kinase inhibition with Y-27632 in bovine eyes. *Exp Eye Res*. 2008;86:271–281.
55. Tektas OY, Hammer CM, Danias J, et al. Morphologic changes in the outflow pathways of bovine eyes treated with corticosteroids. *Invest Ophthalmol Vis Sci*. 2010;51:4060–4066.
56. Wade NC, Grierson I, O'Reilly S, et al. Cross-linked actin networks (CLANs) in bovine trabecular meshwork cells. *Exp Eye Res*. 2009;89:648–659.
57. Flugel C, Tamm E, Lutjen-Drecoll E. Different cell populations in bovine trabecular meshwork: an ultrastructural and immunocytochemical study. *Exp Eye Res*. 1991;52:681–690.